molecular pharmaceutics

articles

Molecular Dynamics Simulations and Experimental Studies of Binding and Mobility of 7-*tert*-Butyldimethylsilyl-10-hydroxycamptothecin and Its 20(*S*)-4-Aminobutyrate Ester in DMPC Membranes

Tian-Xiang Xiang, Zhi-Qiang Jiang, Lin Song, and Bradley D. Anderson*

Department of Pharmaceutical Sciences, College of Pharmacy, University of Kentucky, Lexington, Kentucky 40506

Received February 3, 2006

Abstract: The enhanced permeability and retention of liposomes in solid tumors makes liposomal formulations attractive for the targeting of various antitumor agents. This study explores the binding, orientation, and dynamic properties of a potent topoisomerase I inhibitor, 7-*tert*-butyldimethylsilyl-10-hydroxycamptothecin (DB-67), and its 20(*S*)-4-aminobutyrate ester prodrug (DB-67-AB) in DMPC liposomes by molecular dynamics (MD) simulations and experimental studies. MD simulations of an all-atom and fully hydrated liquid-crystalline bilayer (2×36 DMPC lipids) containing single molecules of DB-67 and DB-67-AB were conducted for up to 50 ns. Membrane/water partition coefficients for DB-67 and DB-67-AB vs pH were determined by ultracentrifugation. Fluorescence spectra and/or steady-state anisotropies were measured in various solvents and in DMPC liposomes. Kinetics for the reversible DB-67 lactone ring-opening in the presence and absence of DMPC liposomes were determined by HPLC with fluorescence detection. During the entire simulation time both DB-67 and DB-67-AB were located on the bilayer membrane near the polar ester groups of DMPC. The average depth of penetration for DB-67 and DB-67-AB was similar (12.4−13.2 Å) with the prodrug's protonated amino group strongly solvated by surface water and lipid phosphate groups. Binding and fluorescence experiments revealed only a modest reduction in the binding affinity upon attachment of the ionized 4-aminobutyrate group onto DB-67. The binding microenvironment polarity resembles that of a polar solvent such as EtOH and DMSO. Kinetics experiments confirmed that DB-67 lactone hydrolysis is inhibited in the presence of DMPC liposomes, consistent with the reduced exposure of its lactone ring to water, as observed in the simulations. Both bound DB-67 and bound DB-67-AB have nonrandom orientations and reduced mobility in the membrane, especially for diffusion normal to the bilayer surface, and rotational relaxation, both of which are ≥ 2 orders of magnitude slower than in bulk water. MD simulations correctly predicted the high binding affinities for DB-67-AB to DMPC bilayers, protection of bound DB-67 toward lactone hydrolysis, and the lack of a substantial reduction in binding for the 20(*S*)-4-aminobutyrate prodrug of DB-67.

Keywords: Lipid bilayers; liposomes; camptothecins; DB-67; prodrugs; lactone hydrolysis; molecular dynamics simulation; DMPC; membrane binding; fluorescence; anticancer drugs

Introduction

The camptothecin analogues are a prominent class of anticancer agents that specifically inhibit the activity of DNA topoisomerase I. Two analogues, topotecan and irinotecan, have received FDA approval, and several others are currently in preclinical and clinical development. In patients, camptothecins undergo widespread biodistribution to both tumor and nontumor sites, with the latter frequently resulting in toxicity to healthy tissues. Camptothecins contain a lactone

* Author to whom correspondence should be addressed. Mailing address: Department of Pharmaceutical Sciences, College of Pharmacy, ASTeCC Bldg. Room A323A, University of Kentucky, Lexington, KY 40506. Phone: 859-257-2300 x235. Fax: 859-257-2489. E-mail: bande2@email.uky.edu.

10.1021/mp0600081 CCC: $33.50
Published on Web 08/22/2006

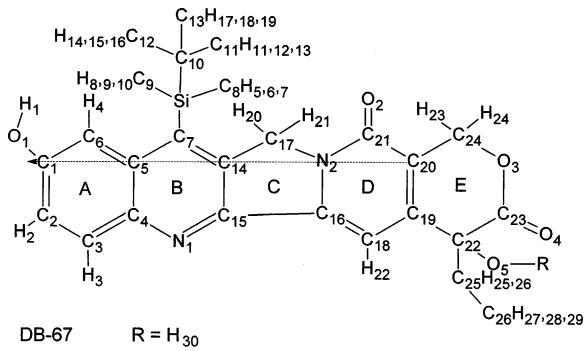

Figure 1. Chemical structures of DB-67 and DB-67-AB, the 20(*S*)-4-aminobutyrate ester of DB-67. The subscript for each atom represents the atom number with the corresponding partial charge listed in Table 1. The arrow represents the vector $\mathbf{V}_{AD}$ connecting the carbon atom that is covalently bonded to the −OH group on the A ring to the carbon atom that is covalently bonded to the carbonyl group on the D ring.

pharmacophore, which undergoes hydrolysis (i.e., ring-opening) at physiological pH to form the inactive carboxylate.[1] For camptothecin itself, the carboxylate form preferentially binds to human albumin, the predominant blood serum protein, thus shifting the lactone/carboxylate equilibrium toward the inactive species.[2,3] The lipophilic silatecan camptothecin analogue 7-*tert*-butyldimethylsilyl-10-hydroxycamptothecin (DB-67; see Figure 1), recently designed by Bom and co-workers,[4,5] exhibits a higher fraction of lactone in the circulation compared to camptothecin and earlier camptothecin analogues. The superior blood stability is the result of decreased albumin binding of the carboxylate and increased binding of the lactone form to lipid bilayers and red blood cell membranes in comparison to camptothecin itself. However, the poor solubility of DB-67 in various solvents and cosolvent systems make its formulation extremely difficult.[6]

The utility of liposomal encapsulation for the effective delivery of anticancer drugs has been affirmed by the FDA approval of liposomal daunorubicin (DaunoXome) and doxorubicin (Doxil). Liposomes themselves are relatively nontoxic and biodegradable, and generally enhance solubility and stability of lipophilic drugs that are unstable in an aqueous environment. Liposomes can accumulate preferentially at tumor sites (i.e., the "enhanced permeability and retention" effect) as a result of their ability to extravasate through "pores" or "defects" in the capillary endothelium, a consequence of the rapid angiogenesis occurring in tumors. Studies have shown that liposomal formulation of topotecan and other camptothecin analogues markedly potentiates their anticancer activities in murine and xenograft models.[7−10] However, the advancement of liposomal camptothecin formulations to the clinic has often been slowed by poor loading and release characteristics, both of which diminish the efficacy of the liposomal drugs. Specifically, the plasma concentration vs time profiles of DB-67 after intravenous administration of DB-67 in solution or in DMPC liposomes were indistinguishable, illustrating the poor retention of DB-67 in liposomes in the circulation (unpublished results). This finding stimulated the exploration of a prodrug approach wherein DB-67 is modified chemically through the attachment of an ionizable moiety to facilitate liposomal retention.[11,12] The 20(*S*)-4-aminobutyrate ester (DB-67-AB; see Figure 1) examined in this study represents a prototype for the prodrug approach. Prodrugs so designed are expected to exhibit improved solubility and retention in liposomes,

(1) Fassberg, J.; Stella, V. J. A kinetic and mechanistic study of the hydrolysis of camptothecin and some analogues. *J. Pharm. Sci.* **1992**, *81* (7), 676−684.

(2) Burke, T. G.; Mishra, A. K.; Wani, M. C.; Wall, M. E. Lipid bilayer partitioning and stability of camptothecin drugs. *Biochemistry* **1993**, *32* (20), 5352−5364.

(3) Burke, T. G.; Mi, Z. The structural basis of camptothecin interactions with human serum albumin: impact on drug stability. *J. Med. Chem.* **1994**, *37* (1), 40−46.

(4) Bom, D.; Curran, D. P.; Kruszewski, S.; Zimmer, S. G.; Thompson Strode, J.; Kohlhagen, G.; Du, W.; Chavan, A. J.; Fraley, K. A.; Bingcang, A. L.; Latus, L. J.; Pommier, Y.; Burke, T. G. The novel silatecan 7-tert-butyldimethylsilyl-10-hydroxycamptothecin displays high lipophilicity, improved human blood stability, and potent anticancer activity. *J. Med. Chem.* **2000**, *43* (21), 3970−3980.

(5) Bom, D.; Curran, D. P.; Zhang, J.; Zimmer, S. G.; Bevins, R.; Kruszewski, S.; Howe, J. N.; Bingcang, A.; Latus, L. J.; Burke, T. G. The highly lipophilic DNA topoisomerase I inhibitor DB-67 displays elevated lactone levels in human blood and potent anticancer activity. *J Controlled Release* **2001**, *74* (1−3), 325−333.

(6) Xiang, T. X.; Anderson, B. D. Stable supersaturated aqueous solutions of silatecan 7-t-butyldimethylsilyl-10-hydroxycamptothecin via chemical conversion in the presence of a chemical modified b-cyclodextrin. *Pharm. Res.* **2002**, *19* (8), 1215−1222.

(7) Emerson, D. L.; Bendele, R.; Brown, E.; Chiang, S.; Desjardins, J. P.; Dihel, L. C.; Gill, S. C.; Hamilton, M.; LeRay, J. D.; Moon-McDermott, L.; Moynihan, K.; Richardson, F. C.; Tomkinson, B.; Luzzio, M. J.; Baccanari, D. Antitumor efficacy, pharmacokinetics, and biodistribution of NX-211: A low-clearance liposomal formulation of lurtotecan. *Clin. Cancer Res.* **2000**, *6*, 2903−2912.

(8) Emerson, D. L. Liposomal delivery of camptothecins. *Pharm. Sci. Technol. Today* **2000**, *3* (6), 205−209.

(9) Messerer, C. L.; Ramsay, E. C.; Waterhouse, D.; Ng, R.; Simms, E.-M.; Harasym, N.; Tardi, P.; Mayer, L. D.; Bally, M. B. Liposomal irinotecan: formulation development and therapeutic assessment in murine xenograft models of colorectal cancer. *Clin. Cancer Res.* **2004**, *10* (19), 6638−6649.

(10) Tardi, P.; Choice, E.; Masin, D.; Redelmeier, T.; Bally, M.; Madden, T. D. Liposomal encapsulation of topotecan enhances anticancer efficacy in murine and human xenograft models. *Cancer Res.* **2000**, *60* (13), 3389−3393.

(11) Liu, X.; Lynn, B. C.; Zhang, J.; Song, L.; Bom, D.; Du, W.; Curran, D. P.; Burke, T. G. A versatile prodrug approach for liposomal core-loading of water-insoluble camptothecin anticancer drugs. *J. Am. Chem. Soc.* **2002**, *124* (26), 7650−7651.

(12) Liu, X.; Zhang, J.; Song, L.; Lynn, B. C.; Burke, T. G. Degradation of camptothecin-20(S)-glycinate ester prodrug under physiological conditions. *J. Pharm. Biomed. Anal.* **2004**, *35* (5), 1113−1125.

enabling slow rates of prodrug release in tumors. Those with the appropriate bioconversion rates would thereby generate the active camptothecin lactone species locally within the tumor.

The loading efficiency, solubility, and release characteristics of a given camptothecin analogue or prodrug may be critically dependent on its lipid bilayer binding affinity. The degree of penetration into the membrane interior can also determine the extent to which a camptothecin analogue or prodrug is protected from decomposition reactions (e.g., lactone-ring opening in DB-67, hydrolysis of the DB-67-AB ester side chain, etc.) that can occur in aqueous or biological fluids. Thus, knowledge of the location and orientation of the drug within bilayer membranes may be useful for understanding relationships between chemical structure and drug-loading, retention and release characteristics, and chemical stability.

Molecular dynamics (MD) simulations may help to address some of these questions prior to expensive and time-consuming syntheses and experiments. Though the authors are unaware of any reported MD simulations of camptothecin−lipid bilayer interactions, MD simulation has been increasingly used to explore molecular interactions and associated solvation and dynamic properties in lipid bilayers (for reviews, see La Rocca et al.[13] and Feller[14]).

The main objective of the present study was to explore various binding and dynamics properties of DB-67 and DB-67-AB in a hydrated dimyristoylphosphatidylcholine (DMPC) bilayer using MD simulation and experiments. The simulation work focused on testing the hypothesis that both campothecin derivatives are predominantly bound to a polar region near the bilayer surface with the molecules oriented such that (1) the reactive lactone ring is shielded from water molecules and therefore stabilized toward hydrolysis in liposomes, and (2) prodrugs containing an ionizable moiety such as the DB-67-AB aminobutyrate side chain also exhibit favorable binding to lipid bilayers due to orientiations in which the protonated amino group resides at the bilayer−water interface. The translational and orientational diffusion of these camptothecins in lipid bilayers have been compared with their dynamic properties in bulk water. Fluorescence studies in DMPC liposomes and five solvents varying in polarity were conducted to evaluate the apparent polarity of partitioning domains in the lipid bilayer and thereby reveal the location of the bound camptothecins. Thermodynamic binding experiments were also conducted to evaluate the relative propensities of DB-67 and DB-67-AB to bind to the lipid bilayers, which can shed light on the influence of the aminobutyrate side chain on binding affinity. Finally, kinetic studies were conducted to explore the effects of DMPC liposomes on DB-67 lactone hydrolysis.

(13) La Rocca, P.; Biggin, P. C.; Tieleman, D. P.; Sansom, M. S. P. Simulation studies of the interaction of antimicrobial peptides and lipid bilayers. *Biochim. Biophys. Acta* **1999**, *1462*, 185−200.

(14) Feller, S. E. Molecular dynamics simulations of lipid bilayers. *Curr. Opin. Colloid Interface Sci.* **2000**, *5*, 217−223.

Experimental and Computational Methods

Force Field and Molecular Models. DB-67 and DB-67-AB were built using the xLeap/Amber program.[15] Once constructed, DB-67 was energy minimized by 50 iterations of steepest-descent and conjugate gradient using Sander/Amber before ab initio calculation was conducted using Gaussian 98 at the level of HF/6-31G* to optimize the structures.[16] The electrostatic potentials (ESPs) around the optimized DB-67 structure generated at the level of HF/6-31G* were then used to obtain atomic partial charges for DB-67 by the restricted ESP fitting (RESP) method.[17] The partial charges for DB-67-AB were assumed to be the same as for DB-67 except for the relatively isolated 20(*S*)-4-aminobutyrate side chain, the partial charges of which were obtained from a model compound, the methyl ester of 4-aminobutyric acid (protonated species), following a procedure similar to that described above for DB-67. The partial charges for DMPC were obtained from Chiu et al.[18] For the Si atom in the camptothecins, a van der Waals radius of 2.10 Å,[19] a Si−C bond length of 1.92 Å,[20] and a C−Si−C angle of 109.5° were assigned. Other unknown force-field parameters for the Si atom were adopted from those for an sp^3 carbon atom (atom type CT) as these parameters are expected to have only a minor effect on the molecular structure and intermolecular interactions for the Si atom buried within four

(15) Case, D. A.; Pearlman, D. A.; Caldwell, J. W.; Cheatham, T. E. I.; Ross, W. S.; Simmerling, C.; Darden, T.; Merz, K. M.; Stanton, R. V.; Cheng, A.; Vincent, J. J.; Crowley, M.; Tsui, V.; Radmer, R.; Duan, Y.; Pitera, J.; Massova, I.; Siebel, G. L.; Singh, U. C.; Weiner, P.; Kollman, P. A. *AMBER*, 6th ed.; University of California: San Francisco, 1999.

(16) Frisch, M. J.; Trucks, G. W.; Schlegel, H. B.; Scuseria, G. E.; Robb, M. A.; Cheeseman, J. R.; Zakrzewski, V. G.; Montgomery, J. A., Jr.; Stratmann, R. E.; Burant, J. C.; Dapprich, S.; Millam, J. M.; Daniels, A. D.; Kudin, K. N.; Strain, M. C.; Farkas, O.; Tomasi, J.; Barone, V.; Cossi, M.; Cammi, R.; Mennucci, B.; Pomelli, C.; Adamo, C.; Clifford, S.; Ochterski, J.; Petersson, G. A.; Ayala, P. Y.; Cui, Q.; Morokuma, K.; Malick, D. K.; Rabuck, A. D.; Raghavachari, K.; Foresman, J. B.; Cioslowski, J.; Ortiz, J. V.; Stefanov, B. B.; Liu, G.; Liashenko, A.; Piskorz, P.; Komaromi, I.; Gomperts, R.; Martin, R. L.; Fox, D. J.; Keith, T.; Al-Laham, M. A.; Peng, C. Y.; Nanayakkara, A.; Gonzalez, C.; Challacombe, M.; Gill, P. M. W.; Johnson, B. G.; Chen, W.; Wong, M. W.; Andres, J. L.; Head-Gordon, M.; Replogle, E. S.; Pople, J. A. *Gaussian 98*, revision A.10; Gaussian, Inc.: Pittsburgh, PA, 1998.

(17) Bayly, C. I.; Cieplak, P.; Cornell, W. D.; Kollman, P. A. A well-behaved electrostatic potential based method using charge restraints for deriving atomic charges: The RESP model. *J. Phys. Chem.* **1993**, *97*, 10269−10280.

(18) Chiu, S.-W.; Clark, M.; Balaji, V.; Subramaniam, S.; Scott, H. L.; Jakobsson, E. Incorporation of surface tension into molecular dynamics simulation of an interface: A fluid phase lipid bilayer membrane. *Biophys. J.* **1995**, *69*, 1230−1245.

(19) Bondi, A. van der Waals volumes and radii. *J. Phys. Chem.* **1964**, *68* (3), 441−451.

(20) Budyka, M. F.; Zyubina, T. S.; Zarkadis, A. K. Quantum chemical study of the Si-C bond photodissociation in benzylsilane derivatives: a specific excited-state′ silicon effect. *Theochem* **2004**, *668* (1), 1−11.

adjacent alkyl groups. The force field parameters for the other atoms in the camptothecins and DMPC were obtained from the Amber all-atom *parm99* force field database.[21] A lipid bilayer assembly consisting of 72 DMPC lipids was first built by converting the DPPC bilayer structure provided by Dr. S. E. Feller (http://persweb.wabash.edu/facstaff/fellers/). The bilayer assembly was then hydrated with two slabs of water on both sides of the lipid bilayer. One DB-67 and one protonated DB-67-AB along with an iodide counterion were then placed right outside the two opposing lipid monolayers by excluding those water molecules that were within van der Waals contact distances of the inserted molecules. The bilayer assembly contained 2511 TIP3P water molecules. To compare solvation and dynamic properties in bulk water, two water assemblies were built by soaking one DB-67 or one DB-67-AB + one iodide ion within a box of 961−962 water molecules using xLeap/Amber.

Molecular Dynamics Simulations. The bilayer assembly was first subjected to energy minimization (500 iterations of steepest-descent/conjugate gradient each) to eliminate bad contacts, followed by a 500 ps equilibration dynamics run at 310 K and 1 bar, during which an external harmonic force (1 kcal/Å^2) centered within the headgroup regions of the lipid bilayer was exerted on atom C_{14} in DB-67 and DB-67-AB to speed up their insertion into the membrane. Within the first 50 ps, both solute molecules were found to reside within the lipid bilayer and no great disturbance to the distribution of the headgroup phosphate atoms of the lipid bilayers was graphically observed. After structural properties of the system such as surface density reached a plateau value (3 ns), long dynamic runs up to a total of 50 ns were performed in which DB-67 and DB-67-AB were allowed to move without any external restraints, and the trajectories in this period were saved every 2 ps for subsequent analysis of various structural and dynamics distributions of interest. MD simulations were conducted with Sander 7, in which Newton's equations of motion for all atoms in the assembly were solved using the Verlet leapfrog algorithm with periodic boundary conditions and a time step of 2 fs. All bond lengths involving hydrogen atoms were constrained with the SHAKE algorithm, and the particle mesh Ewald (PME) method was used to calculate electrostatic contributions. An atom-based cutoff of 13 Å was used for the real space part of the Ewald sum and van der Waals interactions. A constant dielectric constant of $\epsilon = 1$ was employed, and the system was maintained at 310 K and 1 bar by loose coupling of the systems to a thermal bath[22] with coupling constants of 1.0 ps. The calculated molecular trajectories were used to examine various structural and dynamics properties of the camptothecins present and related membrane properties using ptraj/Amber or homemade computer codes. Calculations were performed on an HP N-4000 complex and four SGI workstations at the University of Kentucky.

Materials. The synthesis of DB-67 was reported previously.[4] The DB-67-20(*S*)-4-aminobutyrate (DB-67-AB) (trifluoroacetate salt) was synthesized in our laboratories[11,23,24] and was found to be of >98% purity by HPLC and NMR. 1,2-Dimyristoyl-*sn*-glycero-3-phosphatidylcholine (DMPC) was obtained from Avanti Polar Lipids, Inc. (Alabaster, AL) and stored in a freezer. Purified deionized water was prepared using a Milli-Q UV plus purification system (Millipore Co., Bedford, MA). All other reagents were of analytical grade and were used without further purification.

Liposome Preparation. DMPC was dissolved in chloroform, evaporated under a stream of nitrogen gas, vacuum-dried overnight, and hydrated in 0.01 ionic strength buffers[25] (pH 3.1, potassium chloroacetate; pH 4.2−5.3, potassium acetate; pH 6.5−7.4, sodium/potassium phosphate) to a final lipid concentration of 10−16 mM. The vesicles prepared were extruded through a stack of two 100 nm pore size polycarbonate membranes (Nuclepore, Pleasanton, CA) 10 times using a LiposoFast-Pneumatic extruder (Avestin, Canada) to form large unilamellar vesicles (LUVs). Vesicle size was determined by dynamic light scattering (Zetasizer-3000, Malvern Instruments Ltd, Malvern, U.K.). Aliquots of DB-67 or DB-67-AB stock solutions in DMSO (1−3 mM) were added to the liposomal preparations to obtain a final drug concentration of 1−3 μM. These samples were incubated at 37 °C for 2 h before subsequent binding or fluorescence experiments.

Determination of Membrane Binding Constants. LUVs containing DB-67 or DB-67-AB incubated at 37 °C were spun in an Optima L-90K ultracentrifuge (Beckman-Coulter) for 1 h at 37 °C and 50 000 rpm. Aliquots (0.2 mL) of each sample before (C_t) and supernatant (C_s) after ultracentrifugation were withdrawn using a 1 mL Pipetman, weighed, and diluted with 0.8 mL of cold methanol gravimetrically using the *same* pipet tip that was used to withdraw the sample such that the cold methanol could rinse the pipet tip, thereby removing any DB-67 or DB-67-AB adsorbed on the pipet tip. This sample handling method is necessary as the drugs, especially DB-67-AB, were found to adsorb onto many glass and plastic materials. The binding constant was calculated as $(C_t - C_s)/C_sC_L$, where drug (C_t and C_s) and lipid concentration C_L were assayed by HPLC.

Lactone Hydrolysis Kinetics. The kinetics of DB-67 lactone-ring opening were investigated at pH 7.4 in the presence and absence of DMPC liposomes. The reactions

(21) Wang, J. M.; Cieplak, P.; Kollman, P. A. How well does a restrained electrostatic potential (RESP) model perform in calculation conformational energies of organic and biological molecules? *J. Comput. Chem.* **2000**, *12*, 1049−1074.

(22) Berendsen, H. J. C.; Postma, J. P. M.; van Gunsteren, W. F.; DiNola, A.; Haak, J. R. Molecular dynamics with coupling to an external bath. *J. Chem. Phys.* **1984**, *81* (8), 3684−3690.

(23) Bom, D. C.; Burke, T. G. Preparation and formulation of highly lipophilic camptothecin prodrugs for therapeutic use in the treatment of cancer and AIDS. WO 2002062340 A1 20020815, 2002.

(24) Burke, T. G.; Bom, D. C. Engineered liposomal particles containing core-loaded prodrugs for the controlled release of camptothecins. WO 2003043584 A2 20030530, 2003.

(25) Perrin, D. D.; Dempsey, B. *Buffers for pH and Metal Ion Control*; Chapman and Hall: London, 1974.

were initiated by adding 10 μL of DB-67 in DMSO into 1 mL of 0.1 M sodium phosphate buffer with or without liposomes to obtain a DB-67 concentration of 1 μM. Triplicate samples were then incubated at 37 °C, and aliquots (0.1 mL) were withdrawn at various time intervals, diluted immediately with an equal volume of cold acetonitrile, centrifuged at 10 000 rpm for 1 min (liposome samples), and analyzed by HPLC.

Fluorescence Measurements. Fluorescence measurements in various solvents and liposomes were conducted on an SLM model 9850 spectrofluorometer interfaced with an IBM PS/2 computer. The emission spectra were recorded using a xenon lamp at an excitation wavelength of 375 nm and at excitation and emission resolutions of 8 and 4 nm, respectively. The spectra were corrected for background signal using appropriate blanks. The sample of 1 μM DB-67 in hexane was filtered through a 4 mm Gelman Acrodisc filter (0.45 μm) before the fluorescence measurement. Steady-state anisotropy measurements were determined in the "L-format" using an excitation wavelength of 375 nm and a long-pass filter (400 nm cutoff; Oriel Co., Stamford, CT) in the emission pathway. In all fluorescence experiments, drug samples contained 1 μM and samples were contained in a quartz cuvette thermostated at 37 °C and stirred magnetically. Exposure of the samples to the light beam was minimized to prevent photobleaching that can reduce the fluorescence intensity over time.

HPLC Analyses. For the partitioning experiments, DB-67 and DB-67-AB were assayed by HPLC in isocratic mode. The HPLC system consisted of a Discovery C_{18} (5 μm) column (4.6 × 150 mm) and guard column (4.6 × 20 mm) (Supelco, Bellefonte, PA), a Beckman 110 B solvent delivery module (Beckman Instruments, San Ramon, CA), a Rheodyne M7125 injector with a 100 μL injection loop (Rainin Instrument, Woburn, MA), a Waters M2487 dual λ absorbance detector (Water Associates, Milford, MA) set at 375 nm, and an HP 3392A integrator (Hewlett-Packard, Avondale, PA). The mobile phase consisted of 41% (v/v) acetonitrile in 2% (w/v) triethylamine-acetate (pH 5.5). The method was found to be linear in the range of 0.25−5.0 μM (r = 1.00) for DB-67 and 0.25−3.0 μM (r = 1.00) for DB-67-AB. The relative standard deviations of response factors for four injections of a standard solution and a single injection of three independently prepared standards were 0.4% and 1.4%, respectively, for DB-67 and 0.3% and 1.3%, respectively, for DB-67-AB.

DB-67 lactone and carboxylate concentrations during the hydrolysis experiments were analyzed using a Waters Alliance 2690 separation system with a Waters SymmetryC_{18} (5 μm) column (3.9 × 150 mm) and guard column (3.9 × 20 mm) and a mobile phase containing 58% (v/v) acetonitrile in 2% (w/v) triethylamine-acetate (pH 5.5) at a flow rate of 1.0 mL/min. The eluted compounds were detected using a fluorescence detector (Waters M474) at an excitation wavelength of 380 nm and emission wavelength of 560 nm. For DB-67 lactone, the method was found to be linear in the range 0.2−2.0 μM (r^2 = 1.00) and the relative standard deviations of response factors for four injections of a standard solution and a single injection of three independently prepared standards were 0.2% and 1.8%, respectively. The DB-67 carboxylate concentrations were determined from the corresponding peak areas in the kinetic model fitting by using its response factor as an adjustable parameter.

DMPC concentrations were analyzed by HPLC (Waters Alliance 2690 separation system) using an evaporative light-scattering detector (model 85, Sedex, Alfortville Cedex, France). The detector drift tube temperature, N_2 gas pressure, and gain settings were 40 °C, 2.2 bar, and 8, respectively. The separations were performed in the normal phase mode using an Allsphere silica column (15 cm × 4.6 mm, 5 μm, Alltech, Deerfield, IL) with a mobile phase gradient (linear ramps: 0 min (100% A) → 5 min (85% A + 15% B) → 8 min (80% A + 20% B) → 12 min (80% A + 20% B), where solvents A and B contained 80:19.5:0.5 (v/v/v) $CHCl_3$:methanol:ammonium hydroxide and 80:19.5:0.5 (v/v/v) methanol:water:ammonium hydroxide, respectively. The sample injection size was 20 μL. The method was found to be linear over a log−log scale (ln(peak area) = 1.05 ln [L] (μg/mL) + 10.33) and in the DMPC concentration [L] range of 0.028−0.17 mM (r = 0.997). The relative standard deviation of response factors for four injections of the same standard solution was 1.8%.

Results and Discussion

Most experimental studies directed toward the determination of drug distribution between water and lipid membranes do not distinguish between drug that has partitioned into the bilayer interior and that bound to the bilayer surface. Partitioning or binding can be inferred, in some cases, by relying on linear free energy relationships to estimate the relevant partition coefficients using certain organic solvents as reference systems.[26] A more direct approach resorts to fluorescence quenching of a membrane-bound molecule using probes such as nitroxides that are covalently bound to lipids at different depths.[27] However, thermal motion of these probes over a wide region and their disruption of local membrane structure cause uncertainty over the accuracy of predictions.[28] More importantly, these methods are unable to refine atomic-level structures and dynamic processes in lipid membranes that are also crucial to molecular binding, stability, and transport in lipid bilayers. In particular, (1) orientational motions of camptothecins in lipid bilayers could determine the degree of exposure of reactive sites (e.g., lactone carbonyl in DB-67) in these molecules to water

(26) Diamond, J. M.; Katz, Y. Interpretation of nonelectrolyte partition coefficients between dimyristoyl lecithin and water. *J. Membr. Biol.* **1974**, *17*, 121−154.

(27) Kaiser, R. D.; London, E. Location of diphenylhexatriene (DPH) and its derivatives within membranes: comparison of different fluorescence quenching analyses and membrane depth. *Biochemistry* **1998**, *37*, 8180−8190.

(28) Perochon, E.; Lopez, A.; Tocanne, J. F. Polarity of lipid bilayers. A fluorescence investigation. *Biochemistry* **1992**, *31*, 7672−7682.

Table 1. Partial Charges of DB-67 and DB-67-AB Determined by Combined Ab Initio and RESP Calculations

atom	charge	atom	charge	atom	charge	atom	charge
			DB-67				
C1	0.3162	H19	0.0353	H10	0.0657	C24	0.0408
C2	−0.1351	C11	−0.1984	C7	−0.1887	H23	0.1161
C3	−0.2596	H11	0.0353	C14	−0.0654	H24	0.1161
C4	0.3375	H12	0.0353	C15	0.3409	O3	−0.4299
C5	−0.0001	H13	0.0353	N1	−0.4692	C23	0.7844
C6	−0.3597	C12	−0.1984	C17	−0.0349	O4	−0.5807
O1	−0.5952	H14	0.0353	H20	0.1037	C22	0.3113
H1	0.4446	H15	0.0353	H21	0.1037	O5	−0.6315
H2	0.1708	H16	0.0353	N2	−0.0123	H30	0.4210
H3	0.1667	C8	−0.3547	C16	−0.0482	C25	0.0097
H4	0.1741	H5	0.0657	C21	0.4809	H25	0.0366
Si	0.5954	H6	0.0657	O2	−0.6004	H26	0.0366
C10	0.2345	H7	0.0657	C20	−0.0660	C26	−0.2485
C13	−0.1984	C9	−0.3547	C19	−0.1544	H27	0.0680
H17	0.0353	H8	0.0657	C18	−0.1713	H28	0.0680
H18	0.0353	H9	0.0657	H22	0.0981	H29	0.0680
			DB-67-AB				
C27	0.8065	C6	−0.3597	C8	−0.3547	C19	−0.1544
O6	−0.5566	O1	−0.5952	H5	0.0657	C18	−0.1713
C28	−0.2777	H1	0.4446	H6	0.0657	H22	0.0981
H30	0.0983	H2	0.1708	H7	0.0657	C24	0.0408
H31	0.0983	H3	0.1667	C9	−0.3547	H23	0.1161
C29	−0.0166	H4	0.1741	H8	0.0657	H24	0.1161
H32	0.0443	Si	0.5954	H9	0.0657	O3	−0.4299
H33	0.0443	C10	0.2345	H10	0.0657	C23	0.7844
C30	0.0966	C13	−0.1984	C7	−0.1887	O4	−0.5807
H34	0.0935	H17	0.0353	C14	−0.0654	C22	0.3113
H35	0.0935	H18	0.0353	C15	0.3409	O5	−0.3872
N3	−0.3478	H19	0.0353	N1	−0.4692	C25	0.0097
H36	0.3334	C11	−0.1984	C17	−0.0349	H25	0.0366
H37	0.3334	H11	0.0353	H20	0.1037	H26	0.0366
H38	0.3334	H12	0.0353	H21	0.1037	C26	−0.2485
C1	0.3162	H13	0.0353	N2	−0.0123	H27	0.0680
C2	−0.1351	C12	−0.1984	C16	−0.0482	H28	0.0680
C3	−0.2596	H14	0.0353	C21	0.4809	H29	0.0680
C4	0.3375	H15	0.0353	O2	−0.6004		
C5	−0.0001	H16	0.0353	C20	−0.0660		

molecules in the hydration layer; (2) perturbation of local lipid organization by inserted camptothecins could significantly influence the hydration structure of water molecules near or within the membrane surface and thereby their ability to hydrolyze the camptothecins; and (3) the anisotropic mobility and binding free energy of camptothecins in lipid bilayers may play important roles in determining their rates of release from liposomes and rates of encounter with each other (aggregation) or with other membrane components. Computer simulation is probably the only direct method to explore the location of membrane-bound molecules and the atomic-level dynamic processes that underlie membrane binding, molecular stability, and mobility in lipid bilayers.

Structural Properties of the Simulated Camptothecin−Lipid Bilayer System. Table 1 lists the partial charges calculated for DB-67 and DB-67-AB using the combined ab initio and RESP method. During the simulations, the A, B, C, and D rings of both camptothecins were found to lie nearly in the same plane, a feature consistent with the ab initio optimized structures. Figure 2 shows a snapshot of the simulated DMPC bilayer where DB-67 and DB-67-AB are, respectively, located within the left and right leaflets of the bilayer. The packing of the simulated lipid bilayer can be characterized by the lipid surface density, though the presence of DB-67 and DB-67-AB in the membrane makes the evaluation of the surface density less certain because of their different size and shape compared to the lipids and their translational and rotational motions. However, because of their smaller molecular weights (479 and 564, respectively, vs 678 for DMPC) and number (1 molecule of DB-67 and 1 molecule of DB-67-AB vs 72 DMPC molecules), their effects on the surface density are expected to be minor (3.2−4.2% total surface area estimated from the projected cross-sectional areas of the camptothecins onto the bilayer surface). Over the course of the long simulation runs after equilibration, the membrane surface density calculated by ignoring the effects of the camptothecins fluctuated over a narrow range of 61−62 Å^2 per lipid with an average of 61.8 Å^2 per lipid. A lower value would be expected if the effects of the camptothecins present were taken into account. Recent MD simulations of DMPC membranes in a liquid-crystalline phase (30−52 °C) gave values near 57 Å^2 per lipid.[18,29] Experimental studies produced values varying over a wider range of 59−66 Å^2 per lipid depending on the temperature and the technique used in the measurement.[30,31] The bilayer thickness as measured by the average distance between phosphate atoms on the opposing monolayers was determined to be 34.2 Å. This result is slightly lower than the experimental value of 35.3 Å determined by Kucerka et al.[31] at a lower temperature of 30 °C, but adjustment for the temperature difference leads to closer agreement. A similar result (35.0 Å) was also found by Janiak et al.[32]

During the dynamics run, both DB-67 and DB-67-AB were allowed to move freely (i.e., no restraining force was applied) but were subjected to various intermolecular as well as intramolecular interactions. The locations of the camptothecins in the membrane were determined by dividing the system into 100 layers of 0.8 Å width normal to the bilayer surface (*Z*-axis) and calculating the residence probabilities for each camptothecin as a whole (center-of-mass) or certain functional groups in the molecules (e.g., the aminobutyrate group) from the accumulated time the molecule or functional groups spent in various regions divided by the total simula-

(29) Chanda, J.; Bandyopadhyay, S. Distribution of ethanol in a model membrane: a computer simulation study. *Chem. Phys. Lett.* **2004**, *392* (1−3), 249−254.

(30) Nagle, J. F.; Tristram-Nagle, S. Lipid bilayer structure. *Curr. Opin. Struct. Biol.* **2000**, *10* (4), 474−480.

(31) Kucerka, N.; Liu, Y.; Chu, N.; Petrache, H. I.; Tristram-Nagle, S.; Nagle, J. F. Structure of fully hydrated fluid phase DMPC and DLPC lipid bilayers using X-ray scattering from oriented multilamellar arrays and from unilamellar vesicles. *Biophys. J.* **2005**, *88* (4), 2626−2637.

(32) Janiak, M. J.; Small, D. M.; Shipley, G. G. Temperature and compositional dependence of the structure of hydrated dimyristoyl lecithin. *J. Biol. Chem.* **1979**, *254* (*13*), 6068−6078.

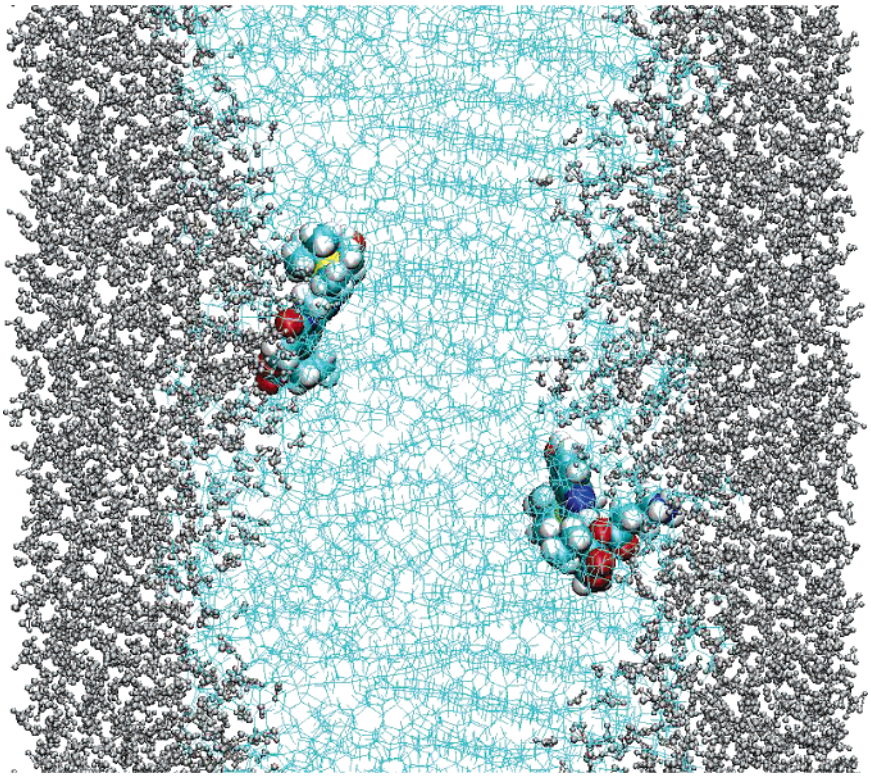

Figure 2. A snapshot of DB-67 (left leaflet) and DB-67-AB (right leaflet) in the hydrated DMPC bilayer. Drawing methods (color keys): DB-67 and DB-67-AB, VDW (white, hydrogen; light blue, carbon; red, oxygen; dark blue, nitrogen; yellow, silicon); H_2O molecules, CPK (silver); and DMPC molecules, lines (light blue).

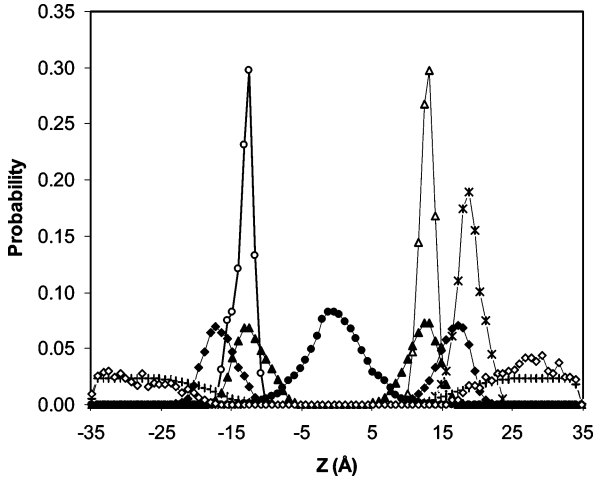

Figure 3. Probability distributions for DB-67 (○) or DB-67-AB (△) as a whole (center-of-mass) and the nitrogen atom of the aminobutyrate group in DB-67-AB (×) versus depth normal to the bilayer surface (*Z*-axis) compared to those for certain lipid groups (phosphate oxygens, ◆; ester carbonyl carbons, ▲; and acyl chain terminal carbons, ●), water molecules (+), and the iodide ion (◇).

tion time. The results are presented in Figure 3 along with those for certain lipid groups, the iodide counterion, and water molecules. The center of the bilayer is located at $Z = 0$ Å. Figure 3 shows that both DB-67 and DB-67-AB reside preferentially near the region frequented by the ester groups of the DMPC lipids where the microenvironment is still polar but exposure to water is greatly diminished (ca. 4−50-fold). The average positions for the centers of mass of DB-67 and DB-67-AB are $|Z| = 12.4$ and 13.2 Å, respectively. However, comparing the distributions using the center of mass of atoms that are present in both molecules yields an almost identical average depth of penetration ($|Z| = 12.4$ and 12.2 Å), suggesting that the presence of the ionic aminobutyrate group in DB-67-AB has only a small impact on the average depth of penetration. Rather, the ionic side chain extends into the headgroup region and the adjacent water layer, where the microenvironment is more polar and can thereby minimize the prodrug's free energy of solvation. On the basis of these results, the ionic aminobutyrate group would be expected to exert a relatively minor influence on the lipid bilayer binding affinity of DB-67-AB.

Radial distribution functions were calculated to gain further insight into the structural properties that affect the drugs' binding and stability in the membrane. Shown in Figure 4 (upper panel) are radial distribution functions, $g(r)$, between the lactone carbonyl carbon in DB-67 or DB-67-AB and surrounding water molecules when the camptothecins were either in the bilayer or in bulk water. The lower panel of Figure 4 shows the radial distribution functions between the positively charged nitrogen atom in DB-67-AB (either in the bilayer or in bulk water) and the oxygen atoms in water molecules or between the positively charged nitrogen atom in bilayer-bound DB-67-AB and certain atoms (e.g., phosphate oxygens and choline nitrogens) in DMPC. From the $g(r)$ between the lactone carbonyl carbon where the ring-

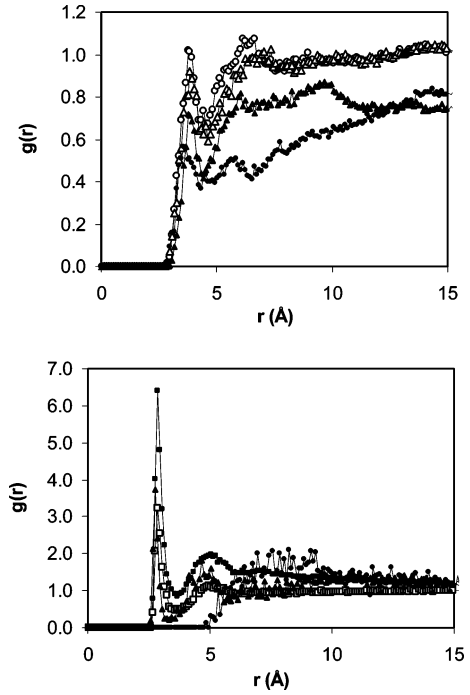

Figure 4. Upper panel: Radial distribution functions, $g(r)$, between the lactone carbonyl carbon in DB-67 (circles) or DB-67-AB (triangles) and water molecules. Lower panel: Radial distribution functions, $g(r)$, for the positively charged nitrogen atom in the aminobutyrate group of bound DB-67-AB with respect to oxygen atoms in water molecules (squares), oxygen atoms in the phosphate groups (triangles), or nitrogen atoms in the choline groups (circles) of the DMPC bilayer. Open symbols, in bulk water; and solid symbols, in the DMPC bilayer.

opening hydrolysis reaction may occur and water molecules (upper panel), it is apparent that the probability of finding a first-shell water (i.e., the first peak at ~2.8−4.3 Å) for the lactone carbonyl carbon in DB-67 bound to the membrane is reduced by about one-half compared with that for the drug in bulk water, while the probability reduction is somewhat less for the prodrug DB-67-AB (~25%). The reduced exposure to water molecules upon binding would be expected to enhance the stability of DB-67 against lactone ring-opening hydrolysis by either water or OH^- ions. Although the distribution of an iodide ion rather than OH^- ions in the lipid bilayer was investigated in this study in an attempt to understand the quenching effects of iodide ions in liposomal systems found in this and other laboratories,[2,33] the OH^- and I^- anions have the same amount of net negative charge that is expected to dominate their interactions with lipid bilayers. As shown in Figure 3, the iodide ion present in the system does not penetrate nearly to the depth where the lactone carbonyl most probably resides (14.8 Å), a result supported by fluorescence quenching experiments (not shown).

(33) Langner, M.; Hui, S. W. Iodide penetration into lipid bilayers as a probe of membrane lipid organization. *Chem. Phys. Lipids* **1991**, *60*, 127−132.

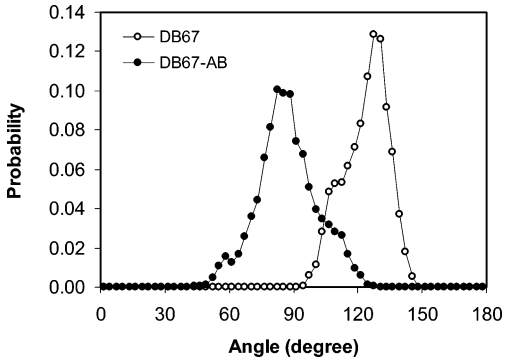

Figure 5. Probability distributions for the orientational angle of the vector $\mathbf{V}_{AD}$ (see Figure 1) passing through the A and D rings of DB-67 (open circles) and DB-67-AB (closed circles) with respect to the normal to the DMPC bilayer surface.

Also evident in Figure 4 (lower panel) is the prominent peak near 2.85 Å (first shell) in the $g(r)$ between the positively charged nitrogen atom in the aminobutyrate group of bound DB-67-AB with respect to oxygen atoms in water molecules. Surprisingly, this peak exceeds that for the corresponding $g(r)$ in bulk water, suggesting that the degree of hydration for this cationic group is not diminished, and may be enhanced, upon binding of DB-67-AB to the membrane. The same aminobutyrate group also interacts favorably with the phosphate oxygens in the polar lipid headgroup. Indeed, the relevant radial distribution functions shown in Figure 4 (lower panel) indicate that the positively charged nitrogen atom in the aminobutyrate group interacts preferentially (i.e., a strong first-shell peak at 2.75 Å in the corresponding $g(r)$) with some of the negatively charged phosphate oxygen atoms in DMPC, whereas the positively charged quaternary ammonium atoms in DMPC appear to be located at a distance from the same nitrogen atom in DB-67-AB (i.e., no first-shell peak and the minimum distance at 5.1 Å) probably due to the unfavorable charge repulsion and the excluded-volume interactions imposed by the three methyl groups covalently attached to the choline nitrogen atom. The above results indicate that the 20(*S*)-4-aminobutyrate group does not appear to substantially diminish the lipid bilayer binding affinity in DB-67-AB.

Because of the ordered nature of the lipid bilayer, the orientations of DB-67 and DB-67-AB in the membrane are not random. Figure 5 shows the orientational distributions for the vector $\mathbf{V}_{AD}$ connecting the carbon atom that is covalently bonded to the −OH group on the A ring and the carbon atom that is covalently bonded to the carbonyl group on the D ring (cf., Figure 1) with respect to the normal to the bilayer surface. On average, the prodrug DB-67-AB is oriented with the $\mathbf{V}_{AD}$ vector almost perpendicular to the bilayer normal (87.3°) while the same vector in DB-67 is tilted more toward the bilayer interior (123.7°). This difference may result from the anchoring effect of the aminobutyrate side chain in DB-67-AB on the bilayer surface.

Dynamic Properties of the Camptothecin Analogues in the Simulated Lipid Bilayer. The dynamic structures of the camptothecins in lipid bilayers and other biological mem-

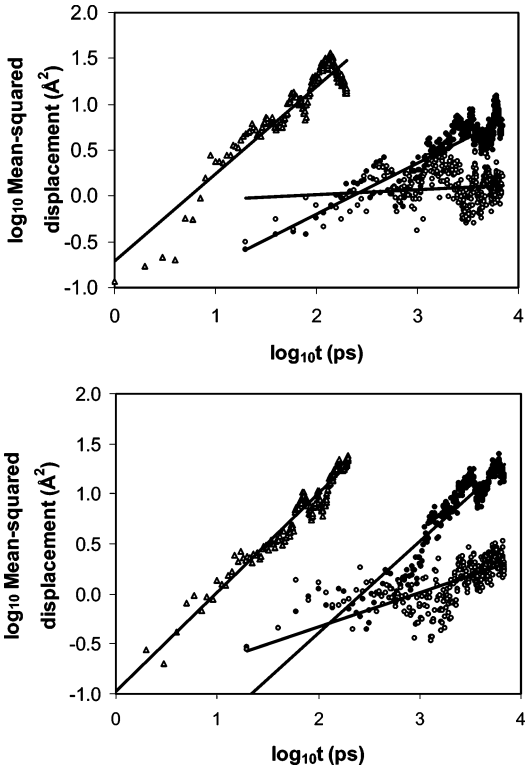

Figure 6. log−log plots of the mean-squared displacements of DB-67 (upper panel) and DB-67-AB (lower panel) versus time. Keys: Δ, $\langle(r_t - r_0)^2\rangle/6$ in bulk water; ●, $\langle(x_t - x_0)^2 + \langle(y_t - y_0)^2\rangle/4$ in the membrane; and ○, $\langle(z_t - z_0)^2\rangle/2$ in the membrane. The lines are the least-squares fits.

branes can be characterized by their translational diffusion coefficients and rotational relaxation times. The diffusion coefficients may be different in the direction normal to (D_z) and in the plane of (D_{x-y}) the membrane surface due to the anisotropic nature of the membranes. D_z is associated with permeability across the membrane while in general D_{x-y} would determine the rates of encounter with other membrane-bound species. In isotropic bulk water, the different components of the diffusion coefficients are identical: $D = D_z = D_{x-y}$. According to the Einstein relation, the overall diffusion coefficient (D) and the different components D_z and D_{x-y} in a condensed phase can be obtained from the mean-squared displacements (MSD):

$$D_z = \frac{1}{2t}\langle(z_t - z_0)^2\rangle \quad (1)$$

$$D_{x-y} = \frac{1}{4t}[\langle(x_t - x_0)^2\rangle + \langle(y_t - y_0)^2\rangle] \quad (2)$$

$$D = \frac{1}{6t}[\langle(r_t - r_0)^2\rangle] \quad (3)$$

where $r_t = \{x_t, y_t, z_t\}$ and $r_0 = \{x_0, y_0, z_0\}$ are sets of molecular Cartesian coordinates at time t and 0, respectively, and the angled brackets represent ensemble averages, or averages over all different time origins t_0 along a molecular trajectory.

Figure 6 shows the log−log plots of the MSD profiles for DB-67 and DB-67-AB in the DMPC bilayer and bulk water. The MSD plots in bulk water and the $x-y$ and z components of the MSD plots in the membrane are divided by a factor of 6, 4, and 2, respectively, for a better visual comparison of the diffusivities in the bulk water and membrane. The diffusion coefficients calculated according to eqs 1−3 are summarized in Table 2. DB-67 has a lower diffusivity than DB-67-AB in the membrane, while in bulk water the larger DB-67-AB has a lower diffusivity. The D_z values for DB-67 and DB-67-AB are about 8−9 times smaller than the corresponding D_{x-y} values in the membrane. Clearly, these camptothecins are more mobile in the plane of the bilayer surface than in the direction normal to the membrane surface. More remarkably, their D_z values in the membrane are 1100 and 330 times smaller than their diffusion coefficients in bulk water. The reduction of diffusivity for smaller solutes (e.g., water, acetamide, benzene, etc.) in a DPPC bilayer were found to be more modest (2−4-fold) in a separate MD study by Bemporad et al.[34] suggesting that the lipid membrane can impose a much larger dynamic barrier to the transport of larger molecules such as DB-67 and DB-67-AB. It should be emphasized that because of the spatially inhomogeneous nature of strong intermolecular interactions near the interface and the short simulation time scale for observation of any excursions of the entire solute into the lipid bilayer interior, the D_z values generated are not a true measurement of the diffusivity in the direction perpendicular to the membrane but rather reflect the net local mobility of the molecules.

Table 2. Structural and Dynamic Properties of DB-67 and DB-67-AB in a Simulated DMPC Bilayer or Bulk Water at 310 K

properties	DB-67	DB-67-AB
position in membrane (Å)[a]		
center-of-mass	12.4	13.2
carbonyl carbon on E ring	14.8	13.0
amino nitrogen on side chain		18.8
D (cm²/s) in water	$(1.5 \pm 0.3) \times 10^{-5}$	$(1.1 \pm 0.1) \times 10^{-5}$
D_z (cm²/s) in membrane	$(1.4 \pm 0.7) \times 10^{-8}$	$(3.3 \pm 1.0) \times 10^{-8}$
D_{x-y} (cm²/s) in membrane	$(1.2 \pm 0.1) \times 10^{-7}$	$(2.9 \pm 0.1) \times 10^{-7}$
τ in water (ps)	$(6.8 \pm 0.8) \times 10^{1}$	$(3.9 \pm 0.2) \times 10^{1}$
τ in membrane (ps)	$(6.7 \pm 0.3) \times 10^{3}$	$(4.6 \pm 0.4) \times 10^{3}$
$1 - c_0$[b]	0.80 ± 0.00	0.68 ± 0.01

[a] Most probable penetration depth. [b] Parameter in eq 5 used for fitting rotational relaxation in the membrane.

Autocorrelation functions (ACF) for the vector $\mathbf{V}_{AD}$ passing through the A and D rings (see Figure 1) in DB-67 and DB-67-AB were calculated to monitor the rotational dynamics of the camptothecin analogues. The ACFs are defined as

$$C(t) = \frac{\langle\vec{m}(0)\cdot\vec{m}(t)\rangle}{\langle m^2(0)\rangle} \quad (4)$$

(34) Bemporad, D.; Essex, J. W.; Luttmann, C. Permeation of small molecules through a lipid bilayer: A computer simulation. *J. Phys. Chem.* **2004**, *108*, 4875−4884.

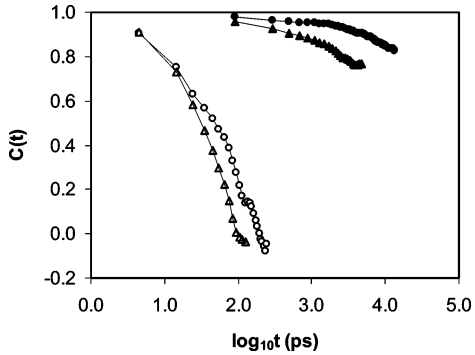

Figure 7. Autocorrelation functions for rotational relaxation of the vector $\mathbf{V}_{AD}$ (see Figure 1) passing through the A and D rings of DB-67 (circles) and DB-67-AB (triangles) in the simulated DMPC bilayer or in bulk water. Open symbols, in bulk water; and solid symbols, in the DMPC bilayer.

where $\vec{m}(t)$ is the vector connecting the atoms of interest and the brackets indicate averages over multiple starting points ($t = 0$) along a molecular trajectory. Figure 7 shows the ACF curves for DB-67 and DB-67-AB in the DMPC bilayer and in bulk water for comparison. The ACFs in bulk water were fitted well ($r = 0.92-0.99$) by a single-exponential function consistent with free rotation, whereas the ACFs in the membrane were better ($r = 1.00$) described by a model of wobbling within a cone angle due to the ordered structure of lipid bilayers:[35]

$$C(t) = c_0\, e^{-t/\tau} + (1 - c_0) \qquad (5)$$

The rotational relaxation times (τ) obtained are presented in Table 2. Most importantly, the relaxation times for both membrane-bound species are 2 orders of magnitude slower than those in bulk water. While relaxation in bulk water was complete in a matter of 0.1−0.2 ns, the same kind of relaxation in the membrane was far from completion even after 20 ns, much longer than a fluorescence lifetime of ca. 4−5 ns found for some camptothecin analogues,[2,36] suggesting a large degree of anisotropy for fluorescence polarization of these compounds in lipid bilayers. The relaxation rates for both membrane-bound and free prodrug DB-67-AB are somewhat higher than those for DB-67.

The fluorescence anisotropy (a) can be described by the Perrin equation:[37]

$$a = a_\infty/(1 + \tau/\phi) \qquad (6)$$

where a_∞ is the limiting fluorescence anisotropy in the absence of depolarizing rotation, τ is the fluorescence lifetime, and ϕ is the rotational relaxation time. Burke and co-workers found that a_∞ is insensitive to camptothecin chemical structure, averaging 0.373 for a variety of camptothecin analogues.[2] Assuming a lifetime of 4−5 ns[2,36] and using the ϕ values obtained in Table 2, a values of 0.23−0.21 and 0.20−0.18 can be estimated for DB-67 and DB-67-AB, respectively. These estimated values are compared with experimental results in the following section.

Experimental Studies. Comparative studies of binding affinity for DB-67 and DB-67-AB to DMPC bilayers were conducted at different pH values. Binding constants (K_m) were defined in terms of a complexation reaction between the drug [D] and lipid molecule [L]:

$$D + L \rightleftharpoons [D-L]$$

or $K_m = [D-L]/[L][D]$, where [L], [D−L], and [D] are the molar concentrations for the lipid and bound and free drug species, respectively. The results, presented in Figure 8, demonstrate that both drug species have similar K_m values (2100−2400 M^{-1}) at neutral pH, while the value of K_m for DB-67-AB decreases at a more acidic pH. The K_m value for DB-67 at pH 7.4, 2200 ± 600 M^{-1}, is close to the value of 2500 M^{-1} obtained by Bom et al.[4] using a fluorescence anisotropy titration method. The modest 2-fold decrease (representing a free energy increase of 0.5 kcal/mol) in K_m for the prodrug is consistent with the finding from the present MD simulations that DB-67-AB resides near the polar ester groups of DMPC with the ionic side chain extended beyond the headgroup region where the solvation of DB-67-AB side chain by water is still largely intact and strong electrostatic interactions with the negatively charged phosphate groups further stabilize the bound drug species. The positive charge on the aminobutyrate group in DB-67-AB would increase the Born solvation energy by about 28 kcal/mol if the entire DB-67-AB molecule were transferred from water (dielectric constant, $\epsilon = 80$) to a nonpolar region ($\epsilon = \sim 2$) in the bilayer interior assuming a Born radius of 3 Å for the charged amine group.[39] This is clearly inconsistent with the experimental binding results, though binding constants among other members of the camptothecin family were found to vary over a much wider range of 10^3-fold.[2,4,40] Using the observed binding constants K_m and the lipid concentration ([L] = 1.6

(35) Engel, L. W.; Prendergast, F. G. Values for and significance of order parameters and "cone angles" of fluorophore rotation in lipid bilayers. *Biochemistry* **1981**, *20*, 7338−7345.

(36) Dey, J.; Warner, I. M., Photophysical properties of camptothecin: Excited-state tautomerization in aqueous solution. In *Book of Abstracts*, 211th National Meeting of the American Chemical Society, New Orleans, LA, March 24−28; American Chemical Society: Washington, DC, 1996; ANYL-062.

(37) van der Meer, B. W.; van Hoeven, R. P.; van Bliterswijk, W. J. Steady-state fluorescence polarization data in membranes. Resolution into physical parameters by an extended Perrin equation for restricted rotation of fluorophores. *Biochim. Biophys. Acta* **1986**, *854*, 38−44.

(38) Leblond-Larouche, L.; Morais, R.; Zollinger, M. Studies of the effect of chloramphenicol, ethidium bromide and camptothecin on the reproduction of Rous sarcoma virus in infected chick embryo cells. *J. Gen. Virol.* **1979**, *44* (2), 323−331.

(39) Jayaram, B.; Sprous, D.; Beveridge, D. L. Solvation free energy of biomacromolecules: Parameters for a modified generalized Born model consistent with the AMBER force field. *J. Phys. Chem.* **1998**, *10*, 9571−9576.

(40) Burke, T. G.; Staubus, A. E.; Mishra, A. K. Liposomal Stabilization of Camptothecin's Lactone Ring. *J. Am. Chem. Soc.* **1992**, *114*, 8318−8319.

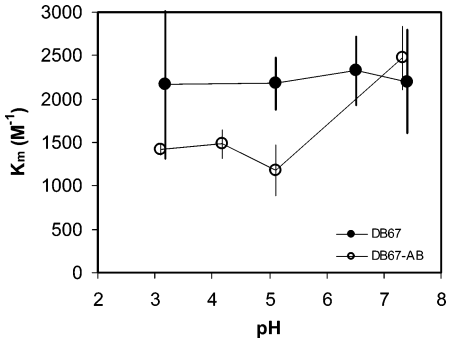

Figure 8. pH dependence of the binding constants (K_m) for DB-67 (●) and DB-67-AB (○) between DMPC LUVs and aqueous solution at 37 °C.

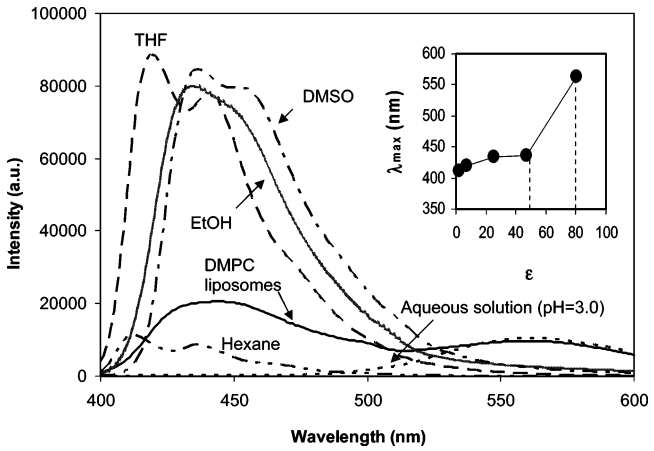

Figure 9. Fluorescence emission spectra of DB-67 (1 μM) at 37 °C and an excitation wavelength of 375 nm in hexane, THF, ethanol, DMSO; 1 mM DMPC LUVs (pH 3.0); and an aqueous PBS solution (pH 3.0). The inset shows the relation between λ_{max} in the emission spectra and the corresponding dielectric constant ϵ in the bulk solvents with the dashed lines corresponding to the interpolated ϵ values predicted from their λ_{max} values in DMPC liposomes.

M) employed in the present MD studies, the probabilities of finding DB-67 and DB-67-AB in a bound state are estimated to be >0.999, which is consistent with the findings in the present MD simulation that both DB-67 and DB-67-AB spent all of their time in a bound state during the entire simulation.

The local environment for DB-67 and DB-67-AB bound onto DMPC membranes can be evaluated by comparing their fluorescence spectra in liposomes with those in solvents of different dielectric constants (i.e., $\epsilon = 80.1$, 47.2, 25.3, 7.52, and 1.9 for water, DMSO, ethanol, THF, and hexane). Figure 9 compares the fluorescence emission spectra for DB-67 in DMPC liposomes, aqueous solution, and various organic solvents. Similar spectral features as described below were also found for DB-67-AB. Several nascent features are noted: (1) There is a large blue shift (560 nm → <420 nm) in the maximum emission intensity (I_{max}) from water to less polar solvents; (2) I_{max} is much larger in a polar organic solvent than in aqueous solution probably due to strong radiationless processes that occur when water molecules are present; and (3) in contrast to emission spectra in organic

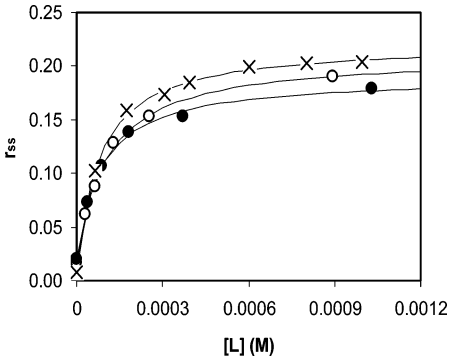

Figure 10. Steady-state fluorescence anisotropies (r_{ss}) for DB-67 and DB-67-AB versus DMPC concentration at 37 °C: ○, DB-67 from the present experiments; ●, DB-67-AB from the present experiments; and ×, DB-67 from an experimental study by Bom et al.[4]

solvents, the fluorescence of DB-67 (or DB-67-AB) in the liposomes exhibits two broad peaks, one near that found in water and the other near that found in a nonaqueous solvent, suggesting that, on the average, the aromatic rings in the camptothecins still have some exposure to water molecules, albeit at a lower level. Indeed, an inspection of the MD snapshots such as that shown in Figure 2 indicated that there were still some water molecules in close proximity to the aromatic rings A−D of DB-67 or DB-67-AB.

The inset in Figure 9 shows the relationship between the maximum emission wavelength (λ_{max}) and solvent polarity (ϵ) for DB-67 compared to the λ_{max} values obtained in DMPC liposomes. Two dashed lines are drawn from the measured λ_{max} values for DB-67 in DMPC membranes since their emission spectra exhibit two peaks. The intercepted ϵ values (~49 and 80) are all much larger than the ϵ value (~2) for a nonpolar solvent such as hexane. Since the bilayer acyl chain region resembles that of a nonpolar hydrocarbon such as hexane, the polar features for the two emission bands found in the liposomes suggest that the nonpolar acyl chain region is not the binding region, consistent with the MD simulations. These experimental results do not enable one to predict the exact location of binding for these camptothecins in the membranes.

Dynamic properties of DB-67 and DB-67-AB in lipid bilayers are reflected in their fluorescence anisotropy. Steady-state anisotropies r_{ss} for DB-67 and DB-67-AB in DMPC liposomes were measured at different lipid concentrations as shown in Figure 10. Extrapolating the r_{ss} profiles in Figure 10 to infinite lipid concentration [L] using an empirical equation, $r_{ss} = a_0 + ac[L]/(1 + c[L])$, which was found to give satisfactory fits ($r = 1.00$) to the anisotropy results in Figure 10, yields anisotropy a values of 0.19 ± 0.01 and 0.17 ± 0.01 for bound DB-67 and bound DB-67-AB, respectively. A separate study by Bom et al.[4] found a slightly higher a value (0.21 ± 0.00) for DB-67. These results agree closely with the a values (0.23−0.21 and 0.20−0.18) obtained in the present MD simulations.

Bom and workers[5] found substantial improvement in hydrolytic stability of the DB-67 lactone ring in the presence

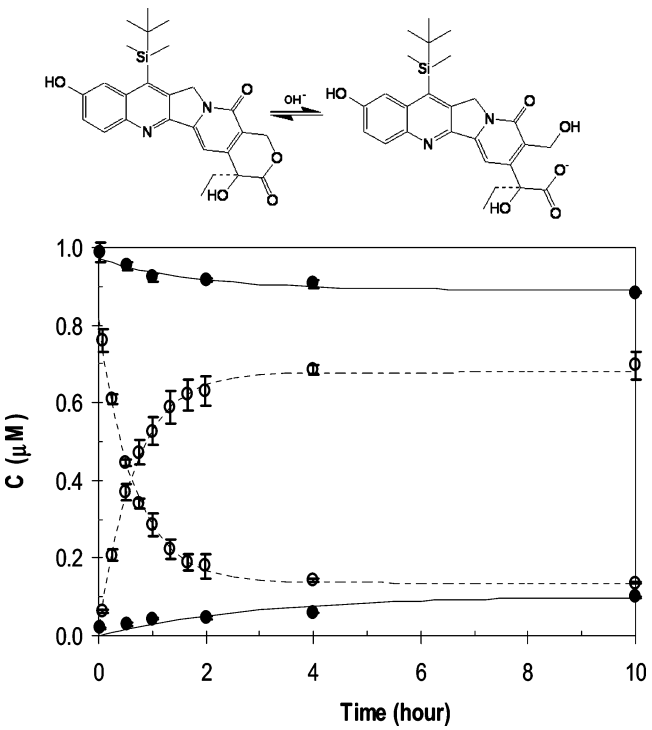

Figure 11. Upper panel: Reversible lactone-ring opening in DB-67. Lower panel: Kinetic profiles for the disappearance of the intact DB-67 lactone and appearance of the ring-opened carboxylate vs time in pH 7.40 buffer in the presence (●) and absence (○) of 14.8 mM DMPC liposomes at 37 °C. The solid curves are least-squares fits using a first-order reversible reaction kinetic model with the forward and reverse rate constants and the response factor for ring-opened DB-67 as adjustable parameters.

of DMPC/DMPG liposomes, though they only followed the disappearance of the intact DB-67 lactone over time and did not apply a kinetic model to their data. In the present study, both the disappearance of the intact DB-67 lactone and the appearance of the ring-opened carboxylate were monitored in 14.8 mM DMPC bilayers over a longer period (10 h) at pH 7.4 to ensure an accurate evaluation of the equilibrium concentrations. The results are presented in Figure 11 (lower panel). As depicted in Figure 11 (upper panel), the reverse reaction is first-order while the second-order forward reaction between the lactone and OH^- ion can be considered to be pseudo-first-order at constant pH. The solid curves in Figure 11 (lower panel) are least-squares fits using Scientist (Micromath Inc., Salt Lake City, UT) and a first-order reversible kinetic model for the conversion of DB-67 from the lactone to the ring-opened carboxylate. The regression analyses yielded pseudo-first-order rate constants for the disappearance of DB-67 lactone and an equilibrium constant (ratio between the pseudo-first-order forward reaction rate constant and the first-order reverse reaction rate constant) between the lactone and carboxylate forms of $1.1 \pm 0.2 \times 10^{-5}$ s^{-1} and 5.2 ± 0.4, respectively, in the presence of the DMPC liposomes, and $3.5 \pm 0.3 \times 10^{-4}$ s^{-1} and 0.12 ± 0.01, respectively, in the absence of liposomes. The results in the absence of the liposomes are close to those ($3.6 \pm 0.1 \times 10^{-4}$ s^{-1} and 0.11 ± 0.00) obtained by Bom et al.[4] The presence of 14.8 mM DMPC in unilamellar vesicles, in which about 97.0% of DB-67 is membrane bound, reduces the forward reaction rate constant by a factor of 31.8 and shifts the equilibrium substantially (43.3-fold) toward the intact lactone, the therapeutically active DB-67 species. This reduction in reaction rate is in qualitative agreement with the conclusions from the present MD simulations that membrane-bound DB-67 has reduced exposure to water, which could protect the lactone carbonyl from attack by water or OH^-.

Conclusions

MD simulations revealed that both DB-67 and its prodrug, DB-67-AB, exhibit high binding affinity for DMPC bilayers. The bound species reside near the polar ester groups of DMPC, and only a small shift (~ 0.8 Å) in binding location occurs upon incorporation of an ionized 20(*S*)-4-aminobutyrate group into DB-67, which is strongly solvated near the bilayer headgroups by surface water and lipid phosphate groups. These results are consistent with binding and fluorescence experiments that found a modest reduction in the binding affinity of DB-67 upon the attachment of this ionic aminobutyrate group and a binding microenvironment having a polarity resembling that of a polar solvent such as DMSO. The MD simulations revealed significantly reduced exposure of the lactone ring in DB-67 to water molecules upon binding in the DMPC bilayer consistent with kinetics experiments that indicated significant stabilization of DB-67 in the presence of DMPC liposomes. Both DB-67 and DB-67-AB have reduced mobility in the lipid bilayer membranes, especially for their diffusion in the direction normal to the bilayer surface, which is >2 orders of magnitude slower than their diffusion in water. Overall, the present MD studies highlight the predictive potential of MD simulations for understanding relationships between structure and drug-loading, retention and release characteristics, and chemical stability.

Acknowledgment. This work was financially supported by grants from the National Cancer Institute (RO1 CA87061-03) and the Kentucky Lung Cancer Research Foundation. The use of the computer resources at the Institute for High Performance Computing and the Center for Computational Sciences, University of Kentucky, is acknowledged. The authors also thank Mr. Stefan Schulz and Ms. Autumn Keller for their contributions to the experimental work.

MP0600081